Scientific Research Publishing

International Journal of Astronomy and Astrophysics, 2021, 11, 59-72
https://www.scirp.org/journal/ijaa
ISSN Online: 2161-4725
ISSN Print: 2161-4717

Adding Dark Matter to the Standard Model

Bruce Hoeneisen

Universidad San Francisco de Quito, Quito, Ecuador
Email: bhoeneisen@usfq.edu.ec

How to cite this paper: Hoeneisen, B. (2021) Adding Dark Matter to the Standard Model. *International Journal of Astronomy and Astrophysics*, **11**, 59-72.
https://doi.org/10.4236/ijaa.2021.111004

Received: December 29, 2020
Accepted: March 2, 2021
Published: March 5, 2021

Abstract

Detailed and redundant measurements of dark matter properties have recently become available. To describe the observations we consider scalar, vector and sterile neutrino dark matter models. A model with vector dark matter is consistent with all current observations.

Keywords

Dark Matter, Boson Dark Matter, Dark Matter Theory, Dark Matter Model

1. Introduction

The Standard Model of quarks and leptons is enormously successful, it has passed many precision tests, and is here to stay. However, if the Standard Model were complete, the universe would have no matter: no dark matter, little baryonic matter, and no neutrino masses. "The New Minimal Standard Model" [1] is an extension that aims to "include the minimal number of new degrees of freedom to accommodate convincing (e.g., $>5\sigma$) evidence for physics beyond the Minimal Standard Model". But this aim has a moving target: as new data becomes available, the model may need to be amended accordingly. The inclusion of a "minimal number of new degrees of freedom" is in accordance with the absence of new particles at the LHC. The purpose of the present study is to see if the New Minimal Standard Model is consistent with the new data on dark matter that has recently become available, and, if necessary, update the model accordingly.

Let us briefly describe the New Minimal Standard Model [1]. First, the Standard Model Lagrangian is extended to include classical gravity. Next, a gauge singlet real scalar Klein-Gordon field with Z_2 parity is added for dark matter. Dark energy is described by the cosmological constant Λ. Two gauge singlet Majorana neutrinos are added to account for neutrino masses and mixing (leaving one neutrino massless until data requires otherwise), and also to obtain ba-

ryogenesis via leptogenesis. Finally, a real gauge singlet scalar field is included to implement inflation.

The outline of this article is as follows. Measurements of dark matter properties are presented in Section 2. Scalar, vector and sterile neutrino dark matter models are studied in Sections 3 to 5. We close with conclusions.

2. Measured Properties of Dark Matter

Fits to spiral galaxy rotation curves [2] [3] [4], and studies of galaxy stellar mass distributions [5] [6] [7], *independently* obtain the following dark matter scenario. Dark matter is in thermal and diffusive equilibrium with the Standard Model sector in the early universe, *i.e.* no freeze-in, and decouples (from the Standard Model sector and from self-annihilation) while still ultra-relativistic, *i.e.* no freeze-out. The decoupling occurs at a temperature $T > T_C \approx 0.2\,\text{GeV}$ to not upset Big Bang Nucleosynthesis. Dark matter has zero chemical potential. The root-mean-square velocity of non-relativistic dark matter particles, at expansion parameter a, is $v_{h\text{rms}}(a) = v_{h\text{rms}}(1)/a$, where $v_{h\text{rms}}(1) = 0.48 \pm 0.19\ \text{km/s}$. Dark matter becomes non-relativistic at an expansion parameter $a'_{h\text{NR}} \equiv v_{h\text{rms}}(1)/c = (1.61 \pm 0.64) \times 10^{-6}$. Dark matter is warm with a free-streaming cut-off wavenumber $k_{\text{fs}} = 0.92^{+0.54}_{-0.24}\,\text{Mpc}^{-1}$. The corresponding free-streaming transition mass is $M_{\text{fs}} \equiv 4\pi(1.555/k_{\text{fs}})^3\,\Omega_m\,\rho_{\text{crit}}/3 = 10^{11.8\pm0.5}\,M_\odot$, comparable with the mass of the Milky Way. The dark matter particle mass is $m_h = 73^{+33}_{-17}$ eV ($m_h = 61^{+28}_{-14}$ eV) for scalar (vector) dark matter. There is evidence in favor of boson dark matter with a significance of 3.5σ [7]. The number of boson degrees of freedom is limited to $N_b = 1$ or 2, *i.e.* to scalar or vector dark matter. The ultra-relativistic dark matter temperature, relative to the photon temperature, after e^+e^- annihilation, is measured to be $T_h/T = 0.456^{+0.039}_{-0.054}$ ($T_h/T = 0.383^{+0.033}_{-0.050}$) for scalar (vector) dark matter. All uncertainties have 68% confidence. These numbers are obtained from Table 4 of [7] for the boson scenario that assumes that non-relativistic dark matter particles reach non-relativistic thermal equilibrium (NRTE) (*i.e.* the non-relativistic Bose-Einstein momentum distribution) due to their dark matter-dark matter elastic scatterings. The relations between $v_{h\text{rms}}(1)$ and m_h and T_h/T for zero chemical potential are [7]:

$$m_h = 51.2\left(\frac{0.76\ \text{km/s}}{v_{h\text{rms}}(1)}\right)^{3/4}\left(\frac{1}{N_b}\right)^{1/4}\text{eV}, \tag{1}$$

$$\frac{T_h}{T} = 0.511\left(\frac{v_{h\text{rms}}(1)}{0.76\ \text{km/s}}\right)^{1/4}\left(\frac{1}{N_b}\right)^{1/4}. \tag{2}$$

In the case of negligible dark matter elastic scattering, the non-relativistic dark matter retains its ultra-relativistic thermal equilibrium (URTE), *i.e.* the ultra-relativistic Bose-Einstein momentum distribution, and the measurements are $v_{h\text{rms}}(1) = 0.67 \pm 0.24\ \text{km/s}$, $a'_{h\text{NR}} = (2.23 \pm 0.80) \times 10^{-6}$, $k_{\text{fs}} = 0.37^{+0.17}_{-0.08}\ \text{Mpc}^{-1}$, $M_{\text{fs}} = 10^{13.0\pm0.4}\,M_\odot$, and $T_h/T = 0.367^{+0.029}_{-0.038}$ ($T_h/T = 0.309^{+0.024}_{-0.033}$) and $m_h = 124^{+50}_{-25}$ eV ($m_h = 104^{+42}_{-21}$ eV) for scalar (vector) dark matter. The relations

between $v_{h\mathrm{rms}}(1)$ and m_h and T_h/T for zero chemical potential are [7]:

$$m_h = 113\left(\frac{0.76\ \mathrm{km/s}}{v_{h\mathrm{rms}}(1)}\right)^{3/4}\left(\frac{1}{N_b}\right)^{1/4}\ \mathrm{eV}, \tag{3}$$

$$\frac{T_h}{T} = 0.379\left(\frac{v_{h\mathrm{rms}}(1)}{0.76\ \mathrm{km/s}}\right)^{1/4}\left(\frac{1}{N_b}\right)^{1/4}. \tag{4}$$

For an overview of these measurements see [8]. To make this article self-contained, **Figure 1** presents forty-six independent measurements of $a'_{h\mathrm{NR}}$ from fits to spiral galaxy rotation curves [4]. From $a'_{h\mathrm{NR}}$ we calculate the warm dark matter free-streaming cut-off wavenumber k_{fs} [7]. This cut-off wavenumber is also obtained from galaxy stellar mass distributions as shown in **Figure 2** [7]. These *independent* measurements are consistent!

The current limit on dark matter self interaction cross-section is $\sigma_{\mathrm{DM\text{-}DM}}/m_{\mathrm{DM}} < 0.47\ \mathrm{cm}^2/\mathrm{g}$ with 95% confidence [14] [15]. A tentative measurement obtains $\sigma_{\mathrm{DM\text{-}DM}}/m_{\mathrm{DM}} \approx (1.7 \pm 0.7)\times 10^{-4}\ \mathrm{cm}^2/\mathrm{g}$ [16]. If this measurement is confirmed, dark matter retains URTE.

The current limits on dark matter particle mass are $m_h > 70\ \mathrm{eV}$ for fermions, and $m_h > 10^{-22}\ \mathrm{eV}$ for bosons [14].

In the present study we will assume this specific dark matter scenario, and ask the following questions. What dark matter interactions lead to this scenario? How is dark matter created? How does dark matter and the Standard Model sector come into thermal and diffusive equilibrium? How do they decouple?

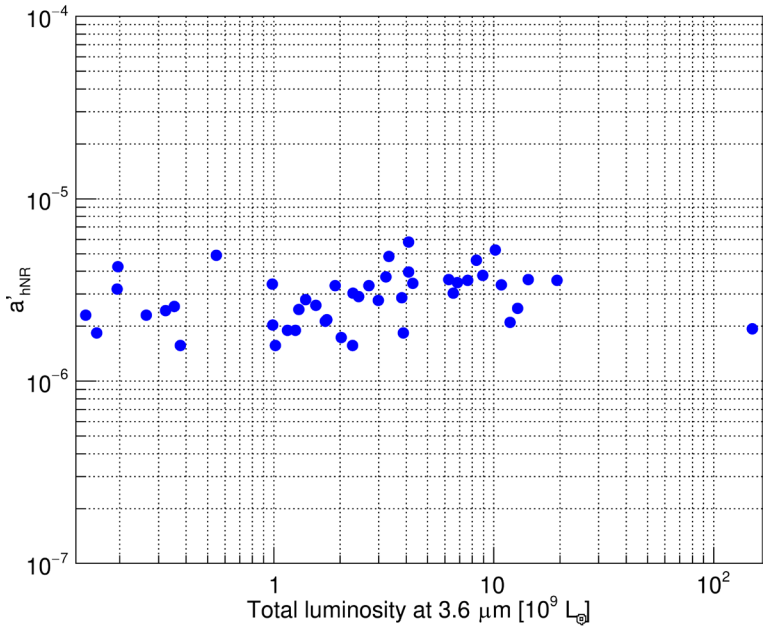

Figure 1. Forty-six independent measurements of the expansion parameter $a'_{h\mathrm{NR}}$ at which dark matter particles become non-relativistic (uncorrected for dark matter halo rotation). Each measurement was obtained by fitting the rotation curves of a spiral galaxy in the Spitzer Photometry and Accurate Rotation Curves (SPARC) sample [9] with the indicated total luminosity at 3.6 μm. Full details of each fit are presented in [4].

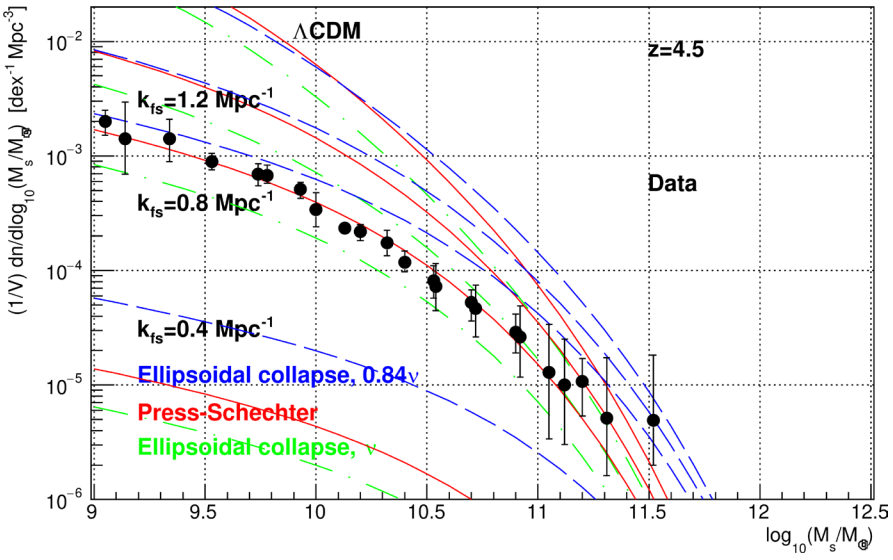

Figure 2. Distribution of stellar masses of galaxies at redshift $z = 4.5$ compared with predictions. From this data, and similar distributions corresponding to $z = 6, 7$, and 8, we obtain the power spectrum cut-off wavenumber $k_{fs} = 0.90^{+0.44}_{-0.40}$ Mpc^{-1}. Figure from [7]. The data are from [10] [11] [12] [13].

How does dark matter acquire mass? Why is dark matter stable (relative to the age of the universe)? And, why is the measured dark matter particle mass m_h so tiny compared to the Higgs boson mass M_H?

Notes: For a discussion of tensions between *measurements* of, and *limits* on, thermal relic dark matter mass see [7] [8]. We should mention that the *observed* galaxy mass distribution presented in **Figure 2** is in tension with Lyman-α forest studies [17]. The 3.5σ confidence in favor of boson dark matter mentioned above, based on spiral galaxy rotation curves and galaxy stellar mass distributions, does not include the Tremaine-Gunn limit on fermion dark matter mass [18] [19]. Including this limit would strengthen the confidence. However, the Tremaine-Gunn limit needs to be revised in view of resent observations on dwarf spheroidal "satellites" of the Milky Way [20] [21] [22] [23].

3. Scalar Dark Matter

The measured dark matter properties allow scalar or vector dark matter, with fermion dark matter disfavored but not ruled out. We begin with the real scalar field S of [1]. To attain thermal and diffusive equilibrium between dark matter and the Standard Model sector we need to add a coupling between the two. The simplest renormalizable coupling is proportional to $(SS)(\phi^\dagger\phi)$ since $(\phi^\dagger\phi)$ is the only Standard Model gauge singlet scalar with mass dimension ≤ 2. ϕ is the Higgs boson field. The interaction rates $\Gamma(SS \leftrightarrow hh)$, relative to the universe expansion rate, scale as $1/T$, so equilibrium is approached towards the future, and statistical equilibrium needs to be achieved by $T \gtrsim M_H$ to avoid freeze-in. Decoupling occurs when the Higgs boson ϕ becomes non-relativistic at $T \approx M_H$. Thereafter the reaction rates become exponentially suppressed be-

cause the Higgs bosons annihilate, and only the tail of the S particle momentum distribution is above threshold. With $M_S < M_H$ there is no freeze-out if S is stable. A super-renormalizable interaction proportional to $S\left(\phi^\dagger\phi\right)$ needs to be avoided because it leads to a ratio of number densities n_S/n_ϕ that depends on T. For this reason, and to obtain a stable S, and to avoid extra parameters in the potential $V(S)$, we impose a Z_2 symmetry $S \leftrightarrow -S$.

Therefore, we consider a gauge singlet real Klein-Gordon scalar dark matter field S, with Z_2 symmetry $S \leftrightarrow -S$, and portal coupling to the Higgs boson [1]. Here we present a brief review of the model to see if it can describe the observed properties of dark matter. To the Standard Model Lagrangian we add

$$\mathcal{L}_S = \frac{1}{2}\partial_\mu S \cdot \partial^\mu S - \frac{1}{2}\bar{m}_S^2 S^2 - \frac{\lambda_S}{4!}S^4 + \cdots, \tag{5}$$

and a contact coupling to the Higgs field ϕ:

$$\mathcal{L}_{S\phi} = -\frac{1}{2}\lambda_{hS}\left(\phi^\dagger\phi\right)S^2. \tag{6}$$

(We are omitting the metric factor $\sqrt{-g}$.) After electroweak symmetry breaking (EWSB) the Higgs doublet, in the unitary gauge, has the form

$$\phi = \begin{pmatrix}\phi^+ \\ \phi^0\end{pmatrix} = \frac{1}{\sqrt{2}}\begin{pmatrix}0 \\ v_h + h(x)\end{pmatrix} \tag{7}$$

with real $h(x)$, the interaction Lagrangian becomes

$$\mathcal{L}_{S\phi} = -\frac{1}{4}\lambda_{hS}\left(v_h^2 + 2v_h h + h^2\right)S^2, \tag{8}$$

and dark matter particles acquire a mass squared

$$M_S^2 = \frac{1}{2}\lambda_{hS}v_h^2 + \bar{m}_S^2 \tag{9}$$

assumed to be >0. We note that S is absolutely stable since there is no interaction term with a single S.

The running of coupling parameters to 1-loop or 2-loop order can be found in [24] [25] [26] [27]. Some center of mass cross-sections are

$$\sigma(hh \leftrightarrow SS) = \frac{\lambda_{hS}^2}{16\pi s}\frac{|\boldsymbol{p}_f|}{|\boldsymbol{p}_i|}, \tag{10}$$

$$\sigma\left(W^-W^+ \leftrightarrow h^* \leftrightarrow SS\right) = \frac{\lambda_{hS}^2 M_W^4}{4\pi s}\frac{|\boldsymbol{p}_f|}{|\boldsymbol{p}_i|}\frac{1}{\left(s - M_H^2\right)^2 + M_H^2\Gamma_H^2}, \tag{11}$$

where $s \equiv (p_1 + p_2)^2$ is the Mandelstam variable. The reaction rates are exponentially suppressed at $T \lesssim M_H$ or $T \lesssim M_W$. These interactions bring dark matter into thermal and diffusive equilibrium with the Standard Model sector at $T \gtrsim M_H$ if $|\lambda_{hS}| \gtrsim 10^{-6}$ and 10^{-6}, respectively. The Higgs boson invisible decay rate for $M_H > 2M_S$ is

$$\Gamma(h \to SS) = \frac{\lambda_{hS}^2 v_h^2}{8\pi M_H}. \tag{12}$$

Requiring this decay rate to be less than the limit on the invisible width of the Higgs boson (≈0.013 GeV [14]) implies $|\lambda_{hS}| \lesssim 0.03$. In summary, we require $10^{-6} \lesssim |\lambda_{hS}| \lesssim 0.03$.

As an example, take $M_S = 73\,\text{eV}$ and $\lambda_{hS} = \pm 10^{-5}$, so $\frac{1}{2}\lambda_{hS} v_h^2 = \pm 0.3\,\text{GeV}^2$. Then there is fine tuning in (9): $\bar{m}_S^2 = 5\times 10^{-15} \mp 0.3\,\text{GeV}^2$. Note that to achieve M_S as low as 73 eV starting from $v_h = 246\,\text{GeV}$ requires fine tuning between two unrelated input parameters with dimensions of mass.

Let us now check whether non-relativistic dark matter acquires the non-relativistic Bose-Einstein momentum distribution due to elastic scattering. The cross-section at $T \ll M_H$ (neglecting interference with (14)),

$$\sigma\left(SS \to h^* \to SS\right) = \frac{9\lambda_{hS}^4 v_h^4}{16\pi s M_H^4}, \tag{13}$$

implies that the mean time between collisions of dark matter particles at $T \lesssim M_S$ is less than the age of the universe even for $\lambda_{hS} = 10^{-6}$, so, in this model, non-relativistic dark matter has non-relativistic thermal equilibrium. The cross-section (neglecting interference with (13)),

$$\sigma\left(SS \to SS\right) = \frac{\lambda_S^2}{16\pi s}, \tag{14}$$

also corresponds to collisional dark matter if $\lambda_S > 10^{-11}$.

Dark matter decouples from the Standard Model sector at $T \approx M_H$ when the Higgs bosons become non-relativistic. As the universe expands and cools, particles and antiparticles that become non-relativistic annihilate heating the Standard Model sector without heating dark matter, or neutrinos if they have already decoupled. For decoupling at M_H we expect the temperature of ultra-relativistic dark matter, relative to the photon temperature, after e^+e^- annihilation, to be $T_h/T = \left[8\times 43/\left(385\times 22\right)\right]^{1/3} = 0.344$ [14], which can be compared with the *measured* ratio $T_h/T = 0.456^{+0.039}_{-0.054}$ [7].

The cross-section limit $\sigma_{\text{DM-DM}}/m_{\text{DM}} < 0.47\,\text{cm}^2/\text{g}$ [14] at $a \approx 1$, and (13), implies $\lambda_{hS} < 5\times 10^{-8}$, so the present model is ruled out. If we lower λ_{hS} to this value, S and the Standard Model sector do not achieve statistical equilibrium at $T \approx M_H$.

4. Vector Dark Matter

To reduce the dark matter-dark matter elastic scattering cross-section, and to relieve the fine tuning in the model of Section 3, we attempt reaching the small m_h in two steps.

To the Standard Model Lagrangian we add a complex scalar field S that is invariant with respect to the local $U(1)_S$ transformation $S \to \exp\left[iQ_S\alpha(x)\right]S$. The corresponding vector gauge boson V^μ acquires mass due to the breaking of the $U(1)_S$ symmetry of the ground state. In the present model, V is the dark matter candidate, and S decays to VV. The dark matter sector is known

in the literature as the "Abelian Higgs model".

The relevant part of the Lagrangian is

$$\mathcal{L}_{\phi SV} = \left(D^{\mu}\phi\right)^{\dagger}\left(D_{\mu}\phi\right) + \left(D'^{\mu}S\right)^{\dagger}\left(D'_{\mu}S\right) - V\left(\phi,S\right), \tag{15}$$

$$V\left(\phi,S\right) = -\mu_h^2\left(\phi^{\dagger}\phi\right) + \lambda_h\left(\phi^{\dagger}\phi\right)^2 - \mu_s^2\left(S^{\dagger}S\right) + \lambda_s\left(S^{\dagger}S\right)^2 + \lambda_{hs}\left(\phi^{\dagger}\phi\right)\left(S^{\dagger}S\right), \tag{16}$$

$$iD_{\mu} = i\partial_{\mu} - g\frac{\boldsymbol{\tau}}{2}\cdot\boldsymbol{W}_{\mu} - g'\frac{1}{2}B_{\mu}, \tag{17}$$

$$iD'_{\mu} = i\partial_{\mu} + g_V Q_S V_{\mu}, \tag{18}$$

$$V_{\mu} \to V_{\mu} + \frac{1}{g_V}\partial_{\mu}\alpha. \tag{19}$$

S and the Standard Model sector have no charges in common.

For $\mu_h^2 > 0$, $\lambda_h > 0$, $\mu_s^2 > 0$, and $\lambda_s > 0$, there is symmetry breaking, and the fields $\phi = \left(h^+, \left(h + iA + v_h\right)/\sqrt{2}\right)^{\mathrm{T}}$ and $S = \left(s + i\rho + v_s\right)/\sqrt{2}$ acquire vacuum expectation values [28]

$$v_h^2 = \frac{2\mu_s^2\lambda_{hs} - 4\mu_h^2\lambda_s}{\lambda_{hs}^2 - 4\lambda_s\lambda_h} \text{ and } v_s^2 = \frac{2\mu_h^2\lambda_{hs} - 4\mu_s^2\lambda_h}{\lambda_{hs}^2 - 4\lambda_s\lambda_h} \tag{20}$$

if $v_h^2 > 0$ and $v_s^2 > 0$. In unitary gauge, the real amplitudes A and ρ become the longitudinal components of Z^{μ} and V^{μ}, respectively, and the complex amplitude $h^{\pm}$ becomes the longitudinal components of W^+ and W^-. The mass eigenstates are

$$M_V = g_V Q_S v_s, \tag{21}$$

$$M_{\phi,S}^2 = \left(\lambda_h v_h^2 + \lambda_s v_s^2\right) \pm \sqrt{\left(\lambda_h v_h^2 - \lambda_s v_s^2\right)^2 + \left(\lambda_{hs} v_h v_s\right)^2}, \tag{22}$$

and the mixing angle is

$$\tan\left(2\theta\right) = \frac{\lambda_{hs} v_h v_s}{\lambda_s v_s^2 - \lambda_h v_h^2}. \tag{23}$$

To bring S into thermal and diffusive equilibrium with the Standard Model sector without exceeding the limit on the invisible width of the Higgs boson h requires $10^{-6} \lesssim \lambda_{hs} \lesssim 0.03$ as in Section 3. Some reactions of interest are

$$\Gamma\left(s \to VV\right) = \frac{g_V^4 Q_S^4 v_s^2}{2\pi M_S}, \tag{24}$$

$$\sigma\left(ss \to h^* \to W^+W^-\right) = \frac{\lambda_{hs}^2 M_W^4}{4\pi s}\frac{\left|\boldsymbol{p}_f\right|}{\left|\boldsymbol{p}_i\right|}\frac{1}{\left(s - M_H^2\right)^2 + M_H^2\Gamma_H^2}, \tag{25}$$

$$\sigma\left(ss \to VV\right) = \frac{g_V^4 Q_S^4}{4\pi s}\frac{\left|\boldsymbol{p}_f\right|}{\left|\boldsymbol{p}_i\right|}. \tag{26}$$

The couplings of V, s, and h (up to order 4) are proportional to h^3, $h^2 s$, hs^2, s^3, h^4, $h^2 s^2$, s^4, $V^2 s$, and $V^2 s^2$. The kinematics allow V to decay only to γ's or ν's. However, we note that there is no coupling with a single V, so V is absolutely stable.

Our challenge is to choose parameters so that S attains statistical equilibrium with the Standard Model sector at $T \gtrsim M_H$, but V does not; and we need the decay $S \to VV$ to occur after S has decoupled from the Standard Model sector, and while S is still ultra-relativistic, *i.e.* within the temperature range $M_S < T < M_H$; and that $m_h = M_V = 112$ eV.

Case $M_S < M_H$**:** Let us assign the high mass eigenstate to ϕ, and the low mass eigenstate to S (the opposite case will be considered below). A particular solution of interest has $|\theta| \ll 1$, so $M_H^2 \approx 2\lambda_h v_h^2 \approx 2\mu_h^2$ as in the Standard Model. A bench-mark scenario with $M_V = 112$ eV is $M_S = 9\times10^{-4}$ GeV, $\lambda_{hs} = 10^{-5}$, $\lambda_s = 0.1$, $g_V Q_S = 6\times10^{-5}$, $v_s = 2\times10^{-3}$ GeV, and $\mu_s = 0.551$ GeV. To meet all requirements, there is fine tuning of μ_s^2 to lower v_s: the relative difference of the two terms in the numerator of (20) is $\approx 10^{-6}$.

The reaction rate of $ss \leftrightarrow h^* \leftrightarrow W^+W^-$, relative to the expansion rate of the universe H, is $1/(\Delta t \cdot H) = 500$ at $T \approx M_H$, so this coupling is strong. For $ss \leftrightarrow hh$, $1/(\Delta t \cdot H) = 700$ at $T \approx M_H$, so this coupling is also strong. For $ss \leftrightarrow VV$, $1/(\Delta t \cdot H) = 3\times10^{-4}$ (200) at $T \approx M_H$ (M_S), so V does not attain statistical equilibrium with S, or with the Standard Model sector, at $T \gtrsim M_H$. The decay rate of $s \to VV$, relative to the expansion rate of the universe H, is $\Gamma(s \to VV)/H = 3\times10^{-7}$ (3×10^4) at $T \approx M_H$ (M_S), so indeed we have arranged that the decay occurs after S has decoupled, and while S is still ultra-relativistic, *i.e.* in the temperature range $M_S < T < M_H$.

The cross-section for $VV \to s^* \to VV$ at $T \ll M_S$ is

$$\sigma(VV \to s^* \to VV) = \frac{9 g_V^8 Q_S^8 v_s^4}{\pi s M_S^4}. \tag{27}$$

This cross-section implies that the mean dark matter particle interaction rate is much less than the expansion rate of the universe H at all temperatures, so, in this model, non-relativistic dark matter retains the ultra-relativistic Bose-Einstein momentum distribution.

The two V's in the decay $S \to VV$ have correlated polarizations, so the average number of boson degrees of freedom, needed to calculate the dark matter density (see (21) of [7]) is $N_{bV} = (2+1)/2$. Then, from (3) and (4), the measured values for this scenario are $m_h \equiv M_V = 112^{+45}_{-23}$ eV, and $T_h/T = 0.332^{+0.026}_{-0.029}$.

For zero chemical potential, the number of s per unit volume, given by the ultra-relativistic Bose-Einstein distribution, is

$$n_s = \frac{N_{bs}}{(2\pi\hbar)^3} \int_0^\infty \frac{4\pi p^2 \mathrm{d}p}{\exp\left[\frac{pc}{kT_s}\right] - 1}, \tag{28}$$

where the number of boson degrees of freedom of s is $N_{bs} = 1$. After the decay

$$2n_s = n_V = \frac{N_{bV}}{(2\pi\hbar)^3} \int_0^\infty \frac{4\pi p^2 \mathrm{d}p}{\exp\left[\frac{pc}{kT_V}\right] - 1}. \tag{29}$$

Each s in 8 orbitals of momentum $2p$ decays to two V's corresponding to

one orbital with momentum p, so

$$2n_s = n_V = 2 \cdot 8 \frac{N_{bs}}{(2\pi\hbar)^3} \int_0^\infty \frac{4\pi p^2 \mathrm{d}p}{\exp\left[\frac{2pc}{kT_s}\right] - 1}. \quad (30)$$

Integrating, we obtain $T_V = (4/3)^{1/3} T_s$. So, the predicted ratio is $T_h/T = (4/3)^{1/3} \cdot 0.344 = 0.379$, to be compared with the measured value $T_h/T = 0.332^{+0.026}_{-0.029}$.

The cross-section limit $\sigma_{\text{DM-DM}}/m_{\text{DM}} < 0.47\ \text{cm}^2/\text{g}$ [14] at $a \approx 1$, and (27), implies $g_V Q_S < 4.3 \times 10^{-4}$, in agreement with the benchmark solution. The tentative measurement $\sigma_{\text{DM-DM}}/m_{\text{DM}} \approx (1.7 \pm 0.7) \times 10^{-4}\ \text{cm}^2/\text{g}$ [16], if confirmed, would imply $g_V Q_S \approx 1.6 \times 10^{-4}$, which is in agreement with the benchmark solution within uncertainties!

In summary, the vector model with $M_S < M_H$ is consistent with all currently measured properties of dark matter. There is fine tuning to obtain the small required symmetry breaking of the ground state of S.

Case $M_S > M_H$**:** Let us now assign the high mass eigenstate to S, and the low mass eigenstate to ϕ. Again, as an example, we consider the case $|\theta| \ll 1$, so $M_H^2 \approx 2\lambda_h v_h^2 \approx 2\mu_h^2$ as in the Standard Model, and $M_S^2 \approx 2\lambda_s v_s^2 \approx 2\mu_s^2$. A benchmark solution with $M_V = 112\ \text{eV}$ is $M_S = 135\ \text{GeV}$, $\lambda_{hs} = 3 \times 10^{-5}$, $\lambda_s = 0.1$, $g_V Q_S = 4 \times 10^{-10}$, $v_s = 300\ \text{GeV}$, and $\mu_s = 96\ \text{GeV}$. When particles S become non-relativistic at $T \approx M_S > M_H$, they decay mostly to the Standard Model sector: reactions $ss \to h^* \to W^+W^-$ are much faster than the universe expansion rate, while $ss \to VV$ and $s \to VV$ are much slower, so the universe is left with no dark matter.

Assigning charges Q_S to Standard Model particles, to enhance or replace the contact interaction between S and ϕ, does not lead to compelling alternative models.

5. Sterile Neutrino Dark Matter

Observations of spiral galaxy rotation curves and of galaxy stellar mass distributions favor boson over fermion dark matter with a significance of 3.5σ [7], so we should not yet rule out fermion dark matter. Sterile neutrinos have been studied extensively as dark matter candidates [29] [30] [31]. In this section we briefly review sterile neutrinos and see if they are consistent with the measured properties of dark matter presented in Section 2.

We extend the Standard Model with a gauge singlet neutrino ν_R with a Majorana mass $M = 107^{+36}_{-20}\ \text{eV}$. This is the *measured* mass for the case of fermion dark matter retaining ultra-relativistic thermal equilibrium (URTE), see Table 4 of [7]. We will refer to the two irreducible representations of the proper Lorentz group of dimension 2 as "Weyl_L" and "Weyl_R". For simplicity we focus on one generation. ν_L and ν_R are two-component Weyl_L and Weyl_R fields, respectively. $i\sigma_2 \nu_L^*$ and $i\sigma_2 \nu_R^*$ transform as Weyl_R and Weyl_L fields, respectively, where σ_2 is a Pauli matrix. $\nu_L^\dagger \nu_R$, $\nu_R^\dagger \nu_L$, $\nu_R^{\mathrm{T}} \sigma_2 \nu_R$, and $\nu_R^\dagger \sigma_2 \nu_R^*$

are scalars with respect to the proper Lorentz group.

To include Weyl spinors into the Standard Model, it is convenient to use 4-component Dirac spinor notation. Our metric is $diag\left(\eta^{\mu\nu}\right)=(1,-1,-1,-1)$. The matrices A and C are defined, in any basis, as $A\gamma_\mu=\gamma_\mu^\dagger A$, and $\gamma_\mu C=-C\gamma_\mu^{\mathrm{T}}$ [31], with $A^\dagger=A$, $C^{\mathrm{T}}=-C$, and $CA^*C^*A=1$. We define $\tilde{\psi}\equiv\psi^\dagger A$, and the charge conjugate field $\psi^c\equiv C\tilde{\psi}^{\mathrm{T}}$. Then $\left(\psi^c\right)^c=\psi$, and $\tilde{\psi}^c=-\psi^{\mathrm{T}}C^{-1}$. A Dirac spinor that satisfies $\psi^c=\mathrm{e}^{i\xi}\psi$ is a Majorana spinor (ξ is an arbitrary phase).

In a Weyl basis [30], $\psi^c=-i\gamma^2\psi^*$, $A=\gamma^0$,

$$\psi=\begin{pmatrix}\nu_L\\ \nu_R\end{pmatrix},\quad \tilde{\psi}=\left(\nu_R^\dagger,\nu_L^\dagger\right), \tag{31}$$

$$\gamma^0=\begin{pmatrix}0&\sigma_0\\ \sigma_0&0\end{pmatrix},\quad \gamma^k=\begin{pmatrix}0&\sigma_k\\ -\sigma_k&0\end{pmatrix},\quad C=\begin{pmatrix}-i\sigma_2&0\\ 0&i\sigma_2\end{pmatrix}, \tag{32}$$

$$\gamma^5=\begin{pmatrix}-\sigma_0&0\\ 0&\sigma_0\end{pmatrix},\quad \psi_L=\begin{pmatrix}\nu_L\\ i\sigma_2\nu_L^*\end{pmatrix},\quad \psi_R=\begin{pmatrix}-i\sigma_2\nu_R^*\\ \nu_R\end{pmatrix}. \tag{33}$$

Note that $\psi_L^c=\psi_L$, and $\psi_R^c=\psi_R$, so these are Majorana fields. With this notation the Majorana fields ψ_L and ψ_R^c can mix. Note however that ψ_L and ψ_R^c are distinct: ψ_L has weak interactions while ψ_R^c does not. $\tilde{\psi}_R\psi_R$, $\tilde{\psi}_L^c\psi_R^c$, $\tilde{\psi}_R\psi_L$, $\tilde{\psi}_R^c\psi_R$, and $\tilde{\psi}_R^c\psi_R^c$ are scalars with respect to the proper Lorentz group. The neutrino mass term after electroweak symmetry breaking has the form [31]

$$\mathcal{L}_{\nu mass}=-\frac{m}{2}\tilde{\psi}_L^c\psi_R^c-\frac{m}{2}\tilde{\psi}_R\psi_L-\frac{M}{2}\tilde{\psi}_R\psi_R^c+H.c., \tag{34}$$

where $m=Yv_h/\sqrt{2}$ is a Dirac mass (Y is a Yukawa coupling), and M is a Majorana mass. We consider the case $|m/M|\ll 1$. The mass eigenstates are [31]

$$\begin{aligned}\psi_{\mathrm{a}}&=i\cos\theta\psi_L-i\sin\theta\psi_R^c,\quad \text{with mass } m_{\mathrm{a}}=\frac{m^2}{M},\\ \psi_{\mathrm{s}}&=\sin\theta\psi_L+\cos\theta\psi_R^c,\quad \text{with mass } m_{\mathrm{s}}=M,\end{aligned} \tag{35}$$

where $\tan(\theta)=m/M$, $\nu_{La}(t)=\nu_{La}(0)\exp\left[\mp iEt\pm i\sqrt{E^2-m_a^2}x\right]$, and $\nu_{Rs}(t)=\nu_{Rs}(0)\exp\left[\pm iEt\mp i\sqrt{E^2-M^2}x\right]$.

Let us now consider dark matter production. We are interested in the reactions $\nu_e e^+\to W^{+*}\to\nu_s e^+$, or $u\bar{u}\to Z^*\to\nu_s\nu_e$. First, we verify that the produced ψ_L is a coherent superposition of ψ_{a} and ψ_{s}. The coherence factor is [32]

$$\varepsilon_{\mathrm{coh}}=\exp\left[-\Delta M^2/\left(8\sigma_E^2\right)\right]\cdot\exp\left[-\Delta t^2/t_{\mathrm{coh}}^2\right], \tag{36}$$

with $\Delta M^2\equiv M^2-m_a^2$. Since we are interested in energy E of ν_L of order $M_W/2$, we take its uncertainty to be $\sigma_E\approx\Gamma_W\gg M$, so the first factor is 1. Δt is the mean time between ν_L interactions. The propagation time of ν_a and ν_s over which their wave packets cease to overlap is the decoherence time [32]

$$t_{\text{coh}} = 2\sqrt{2}\,\frac{2E^2}{\left|\Delta M^2\right|}\sigma_t. \tag{37}$$

Taking the wave packet duration $\sigma_t \approx 1/\Gamma_W$, we estimate $\Delta t \ll t_{\text{coh}}$ for the small value of M being considered. In conclusion, $\varepsilon_{\text{coh}} \approx 1$, and ν_a and ν_s do not become decoherent between ν_L interactions, so we must take into account their oscillations.

Consider initial conditions for ψ_L production to be $\psi_L(0) \propto 1$ and $\psi_R^c(0) \propto 0$. Then, from (35), we obtain the probabilities $P_L(\Delta t) = \left|\psi_L(\Delta t)\right|^2$ to observe a Weyl_L neutrino, and $P_s(\Delta t) = \left|\psi_R^c(\Delta t)\right|^2$ to create a sterile neutrino,

$$P_s(\Delta t) = 1 - P_L(\Delta t) = 4\sin^2\theta\cos^2\theta\sin^2\left(\frac{\Delta M^2}{4E}x\right), \tag{38}$$

with $x \approx \Delta t$, and $E = \sqrt{s}/2$. Note that $P_s(\Delta t) = 2m_a/M$ for $\Delta M^2 \Delta t/(4E) \gg \pi$, but this probability is suppressed by a factor $2\sin^2\left[\Delta M^2\Delta t/(4E)\right]$ for small Δt. Equation (38) describes the oscillation between the active and sterile neutrinos. Similar phenomenology has been confirmed in neutrino flavor oscillation experiments.

The cross-section $\sigma\left(\nu_e e^+ \to W^{+*} \to \nu_e e^+\right)$ is given by Eq. (50.25) of [14]. Multiplying by $P_s(\Delta t)$ we obtain the cross-section for sterile neutrino production $\sigma\left(\psi_L l^+ \to W^{+*} \to \psi_s l^+\right)$. We find that the production mechanism $\psi_L l^+ \to W^{+*} \to \psi_s l^+$ to bring ν_s into statistical equilibrium with the Standard Model sector at $T \approx M_W$, and decouple at $T \gtrsim 0.2$ GeV, fails because of the interference factor $2\sin^2\left[\Delta M^2\Delta t/(4E)\right] \ll 1$. (Note: In Figure 11 of [2] I did not include this factor so that figure is wrong.)

The production channel $W^+W^- \to h^* \to \psi_L\psi_R$ is negligible.

6. Conclusions

Accurate, detailed and redundant measurements of dark matter properties have recently become available [7]. We have studied scalar, vector and sterile neutrino dark matter models in the light of these measurements. The vector dark matter model presented in Section 4 is (arguably) the renormalizable model with the least number of new degrees of freedom that is consistent with all current observations, and replaces the scalar dark matter model of Section 3 [1] that is ruled out. The sterile neutrino dark matter production mechanism studied in Section 5 did not meet experimental constraints.

New insights pose new questions. If nature has chosen the vector dark matter of Section 4, why do the two terms in the numerator of (20) cancel to 1 part in 10^6? Similar questions can be made regarding the cosmological constant Λ, or the strong CP phase θ. Do the scalars ϕ and/or S participate/cause inflation? Baryogenesis via leptogenesis (arguably) requires sterile Majorana neutrinos. How are they produced? What is the origin, if any, of their masses?

How can we move forward? A signal in direct dark matter searches would rule out the vector model. Indirect searches may find an excess of photons (or neu-

trinos!) with energy ≈36 eV, ≈53 eV, or ≈62 eV, if dark matter is unstable and decays. Such a signal would also rule out the vector dark matter model. Collider experiments may discover an invisible Higgs decay width. Further progress will come from the cosmos: more studies of disk galaxy rotation curves, and galaxy stellar mass distributions (these studies can enhance the boson/fermion discrimination, and perhaps can observe the predicted tail of the boson warm dark matter power spectrum cut-off factor $\tau^2\left(k/k_{\mathrm{fs}}\right)$ [7]), galaxy formation simulations, the "small scale crisis" (missing satellites, too big to fail, galaxy core vs. cusp, large voids), super massive black holes at galaxy centers (Einstein condensation may occur at the galaxy center), revised constraints on fermion dark matter mass from the Tremaine-Gunn limit, and tighter constraints on dark matter self-interactions. It is necessary to understand the tensions between the Lyman-α forest studies and the *observed* galaxy stellar mass distributions, see **Figure 2**. Studies of dark matter halo rotation in disk galaxies are also needed.

Conflicts of Interest

The author declares no conflicts of interest regarding the publication of this paper.

References

[1] Davoudiasl, H., Kitano, R., Li, T. and Murayama, H. (2005) The New Minimal Standard Model. *Physics Letters B*, **609**, 117-123. https://doi.org/10.1016/j.physletb.2005.01.026

[2] Hoeneisen, B. (2019) A Study of Dark Matter with Spiral Galaxy Rotation Curves. *International Journal of Astronomy and Astrophysics*, **9**, 71-96. https://doi.org/10.4236/ijaa.2019.92007

[3] Hoeneisen, B. (2019) A Study of Dark Matter with Spiral Galaxy Rotation Curves. Part II. *International Journal of Astronomy and Astrophysics*, **9**, 133-141. https://doi.org/10.4236/ijaa.2019.92010

[4] Hoeneisen, B. (2019) The Adiabatic Invariant of Dark Matter in Spiral Galaxies. *International Journal of Astronomy and Astrophysics*, **9**, 355-367. https://doi.org/10.4236/ijaa.2019.94025

[5] Hoeneisen, B. (2019) Simulations and Measurements of Warm Dark Matter Free-Streaming and Mass. *International Journal of Astronomy and Astrophysics*, **9**, 368-392. https://doi.org/10.4236/ijaa.2019.94026

[6] Hoeneisen, B. (2020) Cold or Warm Dark Matter?: A Study of Galaxy Stellar Mass Distributions. *International Journal of Astronomy and Astrophysics*, **10**, 57-70. https://doi.org/10.4236/ijaa.2020.102005

[7] Hoeneisen, B. (2020) Fermion or Boson Dark Matter? *International Journal of Astronomy and Astrophysics*, **10**, 203-223. https://doi.org/10.4236/ijaa.2020.103011

[8] Hoeneisen, B. (2020) What Is Dark Matter Made of? *Proceedings of the* 3*rd World Summit on Exploring the Dark Side of the Universe*, Guadeloupe Islands, 9-13 March 2020, 109.

[9] Lelli, F., McGaugh, S.S. and Schombert, J.M. (2016) SPARC: Mass Models for 175 Disk Galaxies with Spitzer Photometry and Accurate Rotation Curves. *The Astronomical Journal*, **152**, 157. https://doi.org/10.3847/0004-6256/152/6/157

[10] Lapi, A., Mancuso, C., Bressan, A. and Danese, L. (2017) Stellar Mass Function of

Active and Quiescent Galaxies via the Continuity Equation. *The Astrophysical Journal*, **847**, 13. https://doi.org/10.3847/1538-4357/aa88c9

[11] Song, M., Finkelstein, S.L., Ashby, M.L.N., *et al.* (2016) The Evolution of the Galaxy Stellar Mass Function at $z = 4$ - 8: A Steepening Low-Mass-End Slope with Increasing Redshift. *The Astrophysical Journal*, **825**, 5. https://doi.org/10.3847/0004-637X/825/1/5

[12] Grazian, A., Fontana, A., Santini, P., *et al.* (2015) The Galaxy Stellar Mass Function at $3.5 \leq z \leq 7.5$ in the CANDELS/UDS, GOODS-South, and HUDF Fields. *Astronomy & Astrophysics*, **575**, A96. https://doi.org/10.1051/0004-6361/201424750

[13] Davidzon, I., Ilbert, O., Laigle, C., *et al.* (2017) The COSMOS2015 Galaxy Stellar Mass Function: 13 Billion Years of Stellar Mass Assembly in 10 Snapshots. *Astronomy & Astrophysics*, **605**, A70. https://doi.org/10.1051/0004-6361/201730419

[14] Zyla, P.A., *et al.* (Particle Data Group) (2020) Review of Particle Physics. *Progress of Theoretical and Experimental Physics*, **2020**, 083C01.

[15] Harvey, D., Massey, R., Kitching, T., Taylor, A. and Tittley, E. (2015) The Non-Gravitational Interactions of Dark Matter in Colliding Galaxy Clusters. arxiv:1503.07675

[16] Massey, R., *et al.* (2015) The Behaviour of Dark Matter Associated with 4 Bright Cluster Galaxies in the 10kpc Core of Abell 3827. *Monthly Notices of the Royal Astronomical Society*, **449**, 3393-3406.

[17] Baur, J., *et al.* (2016) Lyman-Alpha Forests cool Warm Dark Matter. *Journal of Cosmology and Astroparticle Physics*. https://doi.org/10.1088/1475-7516/2016/08/012

[18] Boyarsky, A., Ruchayskiyc, O. and Iakubovskyi, D. (2009) A Lower Bound on the Mass of Dark Matter Particles. *Journal of Cosmology and Astroparticle Physics*. https://doi.org/10.1088/1475-7516/2009/03/005

[19] Tremaine S. and Gunn, J.E. (1979) Dynamical Role of Light Neutral Leptons in Cosmology. *Physical Review Letters*, **42**, 407. https://doi.org/10.1103/PhysRevLett.42.407

[20] Hammer, F., Yang, Y.B., Arenou, F., Puech, M., Flores, H. and Babusiaux, C. (2019) On the Absence of Dark Matter in Dwarf Galaxies Surrounding the Milky Way. *The Astrophysical Journal*, **883**, 171. https://doi.org/10.3847/1538-4357/ab36b6

[21] Hammer, F., Yang, Y., Arenou, F., Wang, J., Li, H., Bonifacio, P. and Babusiaux, C. (2020) Orbital Evidences for Dark-Matter-Free Milky Way Dwarf Spheroidal Galaxies. *The Astrophysical Journal*, **892**, 3. https://doi.org/10.3847/1538-4357/ab77be

[22] Yang, Y., Hammer, F., Fouquet, S., Flores, H., Puech, M., Pawlowski, M.S. and Kroupa, P. (2014) Reproducing Properties of MW dSphs as Descendants of DM-Free TDGs. *Monthly Notices of the Royal Astronomical Society*, **442**, 2419-2433. https://doi.org/10.1093/mnras/stu931

[23] Hammer, F., Yang, Y.B., Arenou, F., Babusiaux, C., Puech, M. and Flores, H. (2018) Galactic Forces Rule the Dynamics of Milky Way Dwarf Galaxies. *The Astrophysical Journal*, **860**, 76. https://doi.org/10.3847/1538-4357/aac3da

[24] Haba, N., Kaneta, K. and Takahashi, R. (2013) Planck Scale Boundary Conditions in the Standard Model with Singlet Scalar Dark Matter. arxiv:1312.2089

[25] Kawana, K. (2019) Multiple Point Principle of the Standard Model with Scalar Singlet Dark Matter and Right Handed Neutrinos. arxiv:1411.2097

[26] Costa, R., Morais, A.P., Sampaio, M.O.P. and Santos, R. (2015) Two-Loop Stability of a Complex Singlet Extended Standard Model. *Physical Review D*, **92**, Article ID: 025024. https://doi.org/10.1103/PhysRevD.92.025024

[27] Costa, R., Morais, A.P., Sampaio, M.O.P. and Santos, R. (2015) Two-Loop Stability of Singlet Extensions of the SM with Dark Matter. arxiv:1504.06421

[28] Chao, W. (2015) First Order Electroweak Phase Transition Triggered by the Higgs Portal Vector Dark Matter. *Physical Review D*, **92**, Article ID: 015025. https://doi.org/10.1103/PhysRevD.92.015025

[29] Profumo, S. (2017) Particle Dark Matter. World Scientific, Singapore.

[30] Schwartz, M.D. (2014) Quantum Field Theory and the Standard Model. Cambridge University Press, Cambridge.

[31] Branco, G.C., Lavoura, L. and Silva, J.P. (1999) CP Violation. Claredon Press, Oxford.

[32] Akhmedov, E. (2019) Quantum Mechanics Aspects and Subtleties of Neutrino Oscillations. *International Conference on History of the Neutrino*, Paris, 5-7 September 2018. arxiv:1901.05232